Bioorganic Chemistry 88 (2019) 102950

Contents lists available at ScienceDirect

Bioorganic Chemistry

journal homepage: www.elsevier.com/locate/bioorg

Synthesis, computational molecular docking analysis and effectiveness on tyrosinase inhibition of kojic acid derivatives

Gülşah Karakaya[a], Aslı Türe[b], Ayşe Ercan[c], Selin Öncül[c], Mutlu Dilsiz Aytemir[a,*]

[a] Department of Pharmaceutical Chemistry, Faculty of Pharmacy, Hacettepe University, Ankara, Turkey
[b] Department of Pharmaceutical Chemistry, Faculty of Pharmacy, Marmara University, İstanbul, Turkey
[c] Department of Biochemistry, Faculty of Pharmacy, Hacettepe University, Ankara, Turkey

ARTICLE INFO

Keywords:
Kojic acid
Mannich reaction
Tyrosinase inhibition
Molecular docking

ABSTRACT

Tyrosinase inhibitors have become increasingly important as whitening agents and for the treatment of pigmentary disorders. In this study, the synthesis of kojic acid derivatives having 2-substituted-3-hydroxy-6-hyroxymethyl/chloromethyl/methyl/morpholinomethylpiperidinyl- methyl/pyrrolidinylmethyl-4*H*-pyran-4-one structure (compounds **1**–**30**) with inhibitory effects on tyrosinase enzyme were described. One-pot Mannich reaction was carried out by using kojic acid/chlorokojic acid/allomaltol and substituted benzylpiperazine derivatives in presence of formaline. Subsequently, cyclic amine (morpholine, piperidine and pyrrolidine) derivatives of the 6th-position of chlorokojic acid were obtained with nucleophilic substitutions in basic medium. The structures of new compounds were identified by FT-IR, ^{1}H- and ^{13}C NMR, ESI-MS and elemental analysis data. The potential mushroom tyrosinase inhibitory activity of the compounds were evaluated by the spectrophotometric method using L-DOPA as a substrate and kojic acid as the control agent. The potential inhibitory activity was also investigated *in silico* using molecular docking simulation method. Tyrosinase inhibitory action was significantly more efficacious for several compounds (IC_{50}: 86.2–362.1 μM) than kojic acid (IC_{50}: 418.2). Compound **3** bearing 3,4-dichlorobenzyl piperazine moiety was proven to have the highest inhibitory activity. The results of docking studies showed that according to the predicted conformation of compound **3** in the enzyme binding site, hydroxymethyl group provides a metal complex with copper ions and enzyme. Thus, this interaction explain the high inhibitory activities of the compounds **1**, **3** and **4** possessing hydroxymethyl substituent supporting the mushroom assay results with docking studies. In accordance with the results, it is suggested that Mannich bases of kojic acid bearing substituted benzyl piperazine groups (compounds **1**, **3**, **4**, **11**, **13**, **14**, **23**, **24**, **28**, and **29**) could be promising antityrosinase agents. Additionally, considering the relationship between tyrosinase inhibitory activity results and molecular docking, a new tyrosinase inhibition mechanism can be proposed.

1. Introduction

Tyrosinase (EC 1.14.18.1), a copper-containing monooxy-genase enzyme, is a key regulatory enzyme widely distributed in nature, that is responsible for the melanin production. Pigmentation of the skin in animals and browning of fruits and vegetables occur by this process [1–3]. When the skin is exposed to excessive levels of UV radiation, hyperpigmentation occurs due to overproduction of melanin and causes several abnormal skin lesions (malign melanoma, hyperpigmentation, melasma, freckles, ephelide, sneile lentigines, etc.) particularly in middle-aged and elderly individuals. Contrarily, if there is no tyrosinase activity in melanocytes, the pigment could not be formed which leads to localized albinism like white spots on the skin of some animals [4]. Furthermore, tyrosinase has shown to be involved in wound healing and contributed to the neurodegeneration associated with Parkinson's disease [5]. Also, melanoma-specific anticarcinogenic activity is also known to be linked with tyrosinase activity [6]. Therefore, the enzymatic activity of tyrosinase has been target for the investigation of inhibitors due to its potential applications in pharmaceutical and cosmetic products. Newly synthesized inhibitors possesing metal chelatig ability and phenolic structure represent the most promising class for tyrosinase inhibitors having similar inhibitory potential as the fungal metabolite kojic acid (5-hydroxy-2-hydroxymethyl-4*H*-pyran-4-one, KA). KA is a well-known antityrosinase agent exhibiting a wide range of pharmacological profile and its antityrosinase potential is mainly attributed to copper-chelating property [2]. However the use of KA in

* Corresponding author at: Hacettepe University, Faculty of Pharmacy, Department of Pharmaceutical Chemistry, 06100 Sihhiye, Ankara, Turkey.
E-mail address: mutlud@hacettepe.edu.tr (M.D. Aytemir).

https://doi.org/10.1016/j.bioorg.2019.102950
Received 17 January 2019; Received in revised form 16 April 2019; Accepted 23 April 2019
Available online 27 April 2019

cosmetics is limited due to its cytotoxicity, chemical instability and low lipophilicity which may result in skin irritations. Thus, it is still great need of developing new tyrosinase inhibitors having optimal hydrophilic and lipophilic character in order to increase dermal penetration without causing adverse reactions. To overcome the problems mentioned, by virtue of its convenient hydroxypyranone skeleton, many KA derivatives have been intensively studied for developing new agents. It can be seen in the literature that aminoacid, peptid, thioether and ester derivatives of KA complexed with metals were synthesized in order to increase the efficacy of tyrosinase inhibitory potential of KA [7–13].

Synthesis of Mannich bases is a well known procedure to gain more lipophilic compounds in organic chemistry. Increasing penetration into the cells are provided by hydrophobic structure. In our laboratory, researches on Mannich bases of KA have been performed for many years [14–19]. Previously, we have reported both the synthesis of new KA derivatives containing the same scaffold presented here and their cytotoxic effects on A375 human malignant melanoma, HGF-1 human gingival fibroblasts, and MRC-5 human lung cell lines by sulphorhodamine B assay. As cytotoxic activity of these compounds against melanoma cells was observed, compounds were found to be significantly more potent than the FDA-approved drugs dacarbazine, temozolomide, and lenalidomide. Results of this study covering anticancer effect and tyrosinase inhibition potential activities were submitted to Turkish and International Patent (TR2017/20155 and PCT/TR2018/050724). Moreover, most of these novel compounds generated under the previous studies of our group desirably represented no harm to healthy cell lines while having killed cancerogenic cell lines. [18]. Also, in one of our recent studies, 3-hydroxy-2-(2,6-dichlorobenzylpiperazin-1-ylmethyl)-6-hydroxymethyl-pyrane-4*H*-one and 3-hydroxy-2-(3,4-dichlorobenzylpiperazin-1-ylmethyl)-6-hydroxymethyl-pyrane-4*H*-one (namely compound **3** in the present study) were synthesized and screened for their antityrosinase, antioxidant, antiaging and antidermatophytic activities. Promising results of the compounds were patented by Aytemir et al. [19].

Hence, as a part of our continuous studies by modifying KA aimed at searching for new effective tyrosinase inhibitors, a total of thirty Mannich bases including seventeen novel compounds with the structure of 2-substituted-3-hydroxy-6-hydroxymethyl/ chloromethyl/methyl/ morpholinylmethyl/piperidinylmethyl/pyrrolidinylmethyl-4*H*-pyran-4-one were synthesized to gain bulky substrats and to contribute a new point of view on the structure-activity relationship of their antityrosinase activity. Structures of the compounds were identified by using FT-IR, ^{1}H NMR, ^{13}C NMR, mass spectroscopy and elementary analysis techniques. Antityrosinase activities of all compounds were determined spectrophotometrically using L-DOPA as substrate.

To achieve more molecular insight, modeling studies were performed to estimate the possible binding conformation of the compounds on the tyrosinase enzyme binding site. Overall; synthesis, antityrosinase activity and molecular modelling results of some novel KA derivatives were studied and presented here.

2. Results and discussion

2.1. Chemistry

In this study, we aimed to synthesize new tyrosinase inhibitors as products of one-pot Mannich reaction. In this concept, KA, chlorokojic acid (5-hydroxy-2-chloromethyl-4*H*-pyran-4-one, CKA) and allomaltol (5-hydroxy-2-methyl-4*H*-pyran-4-one, ALM) were reacted with secondary amines such as morpholine, piperidine, and pyrollidine groups using the methodology represented in Scheme 1.

Treatment of KA with thionylchloride ($SOCl_2$) yielded CKA which following reduction with zinc and HCl yielded ALM. These compounds were used as the initial materials to achieve compounds **1–30**. Mannich bases were prepared with high yields in reaction of appropriately substituted benzylpiperazine derivatives with KA/CKA/ALM and formaline at room temperature by using Method I. The resulting precipitate was collected by filtration and washed with cold methanol. Finally, Mannich bases of CKA reacted with morpholine, piperidine or pyrrolidine moieties to synthesize new compounds with the structure of 2-substituted-3-hydroxy-6-(morpholinylmethyl/piperidinylmethyl/pyrrolidinylmethyl)-4*H*-pyran-4-one by using Method II. Reaction occurred in the aprotic solvent dimethylformamide (DMF) and basic medium provided by K_2CO_3. Formation of the desired novel compounds was confirmed on the basis of elementary analysis and spectroscopic methods. Physical properties of the compounds **1–30** including their molecular formulas, yield of reaction, melting points and clogP values with IC_{50} (μM) results of mushroom tyrosinase inhibition are given in Table 1.

Structures of the synthesized compounds were confirmed by FT-IR, ESI-MS, ^{1}H- and ^{13}C NMR spectroscopy. In the IR spectra of all compounds showed stretching bands associated with (C=O) and (C=C) were observed at about 1620 and 1450 cm^{-1}, respectively. O—H stretching bands were detected around 3330 cm^{-1}. In ^{1}H NMR spectra, aromatic protons were defined between 7.31 and 7.10 ppm. Characteristic H^5 proton of the 4*H*-pyran-4-one ring was determined as singlet peaks at about 6.5 ppm. The ^{13}C NMR spectra of the compounds were also consistent with the proposed structures. The characteristic signal of the ketonic group in the pyranone ring exhibited around 173 ppm. The molecular masses of the compounds were confirmed by electron spray ionization (ESI) mass spectrometry. Distinctive molecular ion peaks equivalent to their molecular formula, quasi molecular ion peaks corresponding to peak of $(M+H)^+$ and sodium peaks $(M^+ + 23)$ were identified in the spectrums. Isotope peaks in the spectra of chlorine atom containing compounds were also observed as well.

While a drug molecule should represent an optimal hydrophilic–lipophilic balance to penetrate into the targeted area, introduction of hydrophobic groups to the molecule increases penetration. It is well known that Mannich bases are used to gain more lipophilic compounds in organic chemistry. Regarding hydrophilicity and lipophilicity of the synthesized compounds, herein, clogP values have been calculated theoretically via ChemDraw Ultra 8.0.3. The clogP values of KA, CKA and ALM are found to be −1.39, 0.21 and 0.15, respectively. After modifying KA structure from the 2nd-position to obtain Mannich bases, clogP values prominently increased and were found in the range of 0.74–1.90. In the next step when morpholine, piperidine and pyrrolidine groups are introduced to the modified KA structure, this value considerably elevated. For instance, clogP of compound **23** bearing 3,4-dichlorobenzyl moiety reached to 3.964.

2.2. Mushroom tyrosinase assay

Generally, two main methods are used to evaluate activity of tyrosinase inhibitors: *in vitro* mushroom tyrosinase assay and cell based assays. Commercially available enzyme is used as a model while performing *in vitro* test. Because of easy-handling application of enzyme, *in vitro* mushroom tyrosinase assay is preferred commonly. It also provides accurate results and allows scientists to work on the enzymological aspects as well [20]. Most importantly, tyrosinase enzyme extracted from mushroom specie of *A. bisporus* is highly homologous with the mammalian ones and assay with *A. bisporus* enzyme is a highly prefered model for studies on melanogenesis [1].

Kinetic study of inhibition of the mushroom tyrosinase activity is quite specific for the substrate. During the evaluation of tyrosinase inhibitory activityof the compounds, method described by Chen [21] was applied with some slight modifications. All compounds were subjected to tyrosinase inhibition assay where L-DOPA was used as a substrate. KA, which is known to inhibit tyrosinase and also starting material for the synthesis process of this study, was used as a positive control. The examined inhibition mechanism was based on *o*-diphenolase activity of tyrosinase. GraphPad Prism 5.03 software was used to determine IC_{50} values and standard deviations. IC_{50} values of the compounds **1–30** as

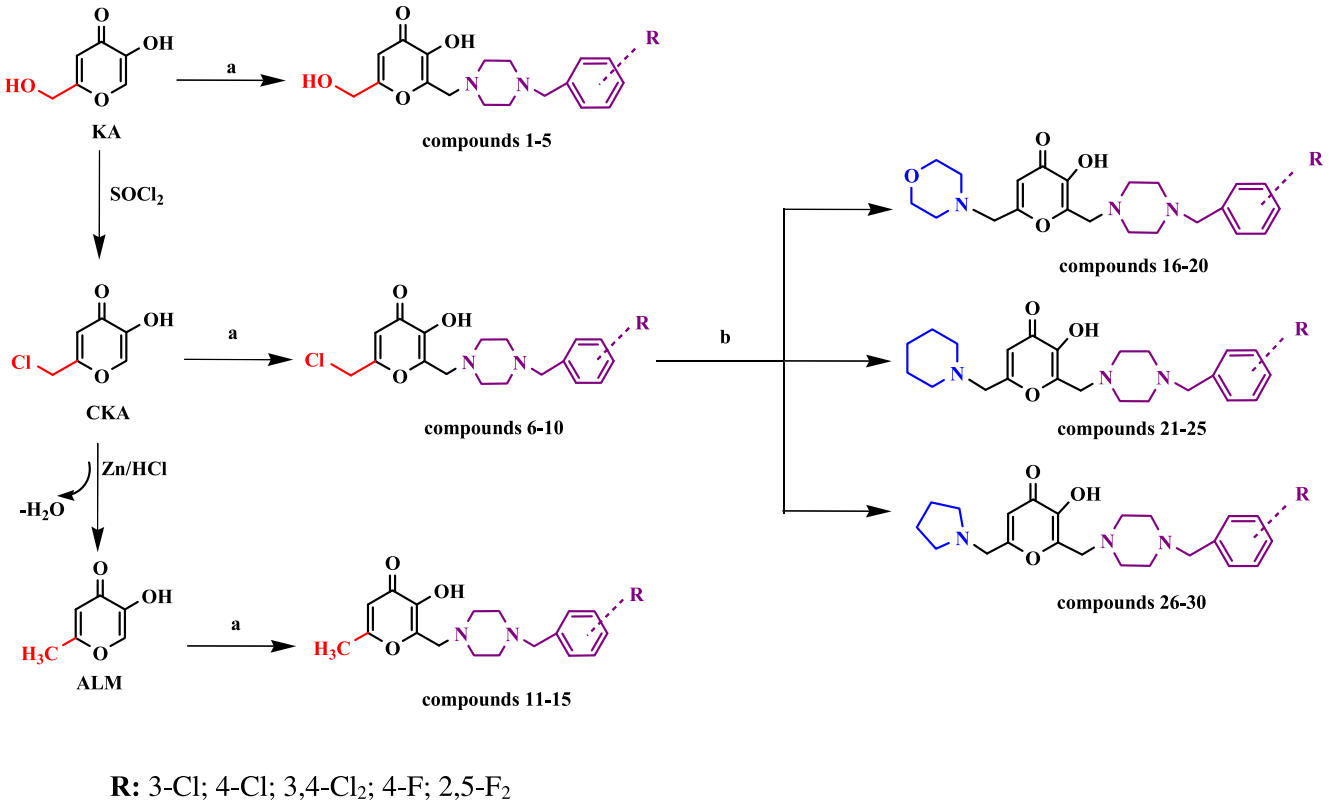

Scheme 1. Synthesis of compounds **1–30**; Reagents and conditions: (a: Method I) substituted benzyl piperazine derivatives, formaline solution 37%, MeOH, rt, (b: Method II) morpholine/piperidine/pyrrolidine, K_2CO_3, DMF, 0 °C; KA: Kojic acid, CKA: Chlorokojic acid; ALM: Allomaltol.

the results of antityrosinase activities were given in Table 1.

Effect of the modification in the 6th-position of pyranone ring on antityrosinase activity was investigated through this study. We first aimed to observe how replacement of hydroxyl moiety of KA with chlorine, hydrogene or some cyclic amine groups (morpholine, piperidine and pyrrolidine) alters antityrosinase activity. For this reason, compunds were generated and screened for their antityrosinase activities. Among them, compounds **3**, **8**, **13**, **18**, **23**, and **28** have common structure of (3,4-dichlorobenzyl)piperazin-1-yl)methyl group at the 2nd-position. These compounds caryy hydroxymethyl, chloromethyl, methyl, morpholinylmethyl, piperidinylmethyl, pyrrolidinylmethyl at the 6th-position on pyranone ring, respectively. As it is stated in Table 1., among these, compound **3** showed the highest inhibitory activity (IC_{50}: 86.2 μM). Assertively, antityrosinase activity of compound **3** was found better than KA (IC_{50}: 418.2 μM) which is the control agent and other starting material in this series. This means, compound **3** showed the antidiphenolase activity of mushroom tyrosinase to be almost 5-fold higher than that of KA. The other compounds in the top-three were compounds **28** and **13** with the IC_{50} values of 94.1 and 123.7 μM, respectively (Scheme 2.). On the contrary, compound **8** had no inhibition over the enzyme. According to the enzymatic assay results, it can be proposed that 3,4-dichlorobenzyl group at the 2nd-position on pyranone ring is important for tyrosinase inhibitory activity. Besides, regarding to enzymatic assay studies, antityrosinase activity is also dependent on the pattern of the 6th-position of pyranone ring.

Among the compounds **1–30**, ten of the Mannich bases (compounds **1**, **3**, **4**, **11**, **13**, **14**, **23**, **24**, **28**, and **29**) showed higher activity than the starting materials ALM (IC_{50}: 411.6 μM), CKA (IC_{50}: 413.7 μM), and KA. Compounds **1**, **29**, **24**, **4**, and **14** had IC_{50} values of 223.2 μM, 225.5 μM, 232.3 μM, 264.2 μM, and 362.1 μM, respectively. While, the common substituent of the compounds **4**, **14**, **24**, and **29** is 4-fluorobenzyl group, compounds **1** and **11** shares 3-chlorobenzyl group in the molecular structure. Changing the number and the position of these substitutions decreased the tyrosinase inhibitory activity. For example, other compounds bearing 4-chloro or 2,5-difluorobenzyl group had lower inhibitory activity compared to starting compounds stated above.

As structures of starting compounds, KA, CKA and ALM, only differ in 6th-position of hydroxypyranone ring; KA, CKA and ALM showed almost equal inhibitory activity toward *o*-diphenolase activity of mushroom tyrosinase. However, when 3-chloro/3,4-dichloro/4-fluoro benzyl moieties are substituted the starting structure via Mannich reaction, inhibition distinctly increased for each starting compounds.

2.3. Molecular modeling studies

Crystal structure of *Agaricus bisporus* tyrosinase enzyme was published in the year of 2011 as tetrameric form consisting of H_2L_2 subunits where active site comprises two copper atoms coordinated by six histidine residues. Two copper ions are present in the native form of protein as well as in the ligand bound form of it. Binuclear copper binding site is surrounded with six conserved histidine residues. Cu-A and Cu-B ions make interactions with His61, His85, His94 and His259, His292, His296, respectively. These interactions limit rotation of histidine residues preventing the flexibility [22]. In order to understand the inhibition of tyrosinase enzyme by KA and the influence of bivalent metal ions, experimental kinetics and computational analysis were studied and published [23]. According to a recent study, substrate binding pocket (six histidine residues along with the binuclear copper ions) surrounded by charged residues such as Glu256 and Glu322 residues of this enzyme is the main binding site for KA [24].

Besides, *Agaricus bisporus* tyrosinase is accessible as native form and tropolone bound form in the Protein Data Bank. Proteins co-crystallized with tropolone as well as KA were derived so that coordinations of tropolone and KA and interactions between these ligands and tyrosinase enzyme were investigated. Fig. 1 shows the coordinations of mentioned ligands in tyrosinase enzymes.

Table 1
Molecular formulas, yields, melting points, clog*P* and IC_{50} (μM) values of mushroom tyrosinase inhibition of the compounds **1–30.**

Comp. No	Structure	Mol. Formula (Mol. Wt. g/mol)	Yield (%)	M.p. (°C)	Clog*P*	IC_{50} (μM)
1	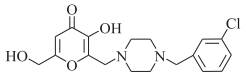	$C_{18}H_{21}ClN_2O_4$ 364.82	91	170–1	1.306	223.2
2	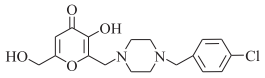	$C_{18}H_{21}ClN_2O_4$ 364.82	96	*Dec.	1.306	710
3[a]	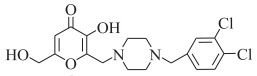	$C_{18}H_{20}Cl_2N_2O_4$ 399.27	90	180–1	1.899	86.2
4	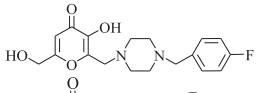	$C_{18}H_{21}FN_2O_4$ 348.37	98	187–8	0.736	264.2
5	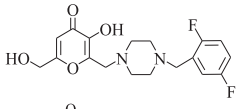	$C_{18}H_{20}F_2N_2O_4$ 366.36	72	176–7	0.879	1564
6	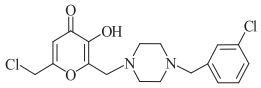	$C_{18}H_{20}Cl_2N_2O_3$ 383.27	76	147–8	2.906	990.7
7[b]	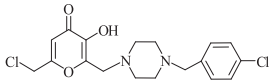	$C_{18}H_{20}Cl_2N_2O_3$ 383.27	92	168–9	2.906	1900
8[c]	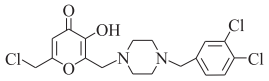	$C_{18}H_{19}Cl_3N_2O_3$ 417.71	90	147–8	3.499	**nd
9[c]	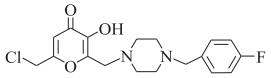	$C_{18}H_{20}ClFN_2O_3$ 366.81	68	157–8	2.336	618.6
10[b]	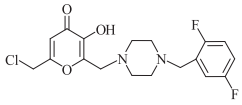	$C_{18}H_{19}F_2N_2O_3$ 384.81	75	151–2	2.479	> 2000
11[***]	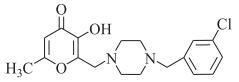	$C_{18}H_{21}ClN_2O_3$ 348.82	63	158–9	2.843	198.7
12[d]	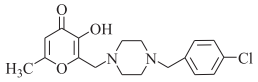	$C_{18}H_{21}ClN_2O_3$ 348.82	75	165–7	2.843	438.8
13[e]	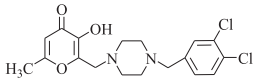	$C_{18}H_{20}Cl_2N_2O_3$ 383.27	60	160–2	3.436	123.7
14	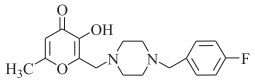	$C_{18}H_{21}FN_2O_3$ 332.37	66	168–70	2.273	362.1
15	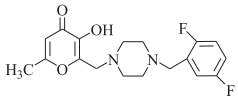	$C_{18}H_{20}F_2N_2O_3$ 350.36	70	163–5	2.416	760.9
16	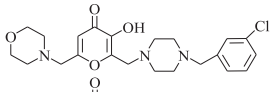	$C_{22}H_{28}ClN_3O_4$ 433.93	13	137–8	2.091	1105
17[e]	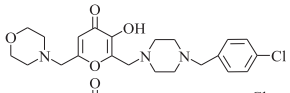	$C_{22}H_{28}ClN_3O_4$ 433.93	46	143–5	2.091	1759
18	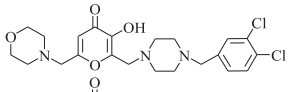	$C_{22}H_{27}Cl_2N_3O_4$ 468.37	12	142–4	2.684	> 2000
19	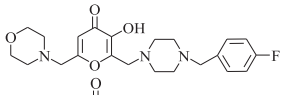	$C_{22}H_{28}FN_3O_4$ 417.47	45	156–7	1.521	1847
20	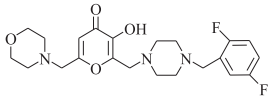	$C_{22}H_{27}F_2N_3O_4$ 435.46	28	107–8	1.664	1900
21	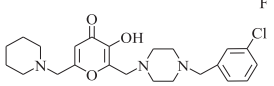	$C_{23}H_{30}ClN_3O_3$ 431.96	58	145–7	3.371	493.8

(*continued on next page*)

Table 1 (*continued*)

Comp. No	Structure	Mol. Formula (Mol. Wt. g/mol)	Yield (%)	M.p. (°C)	Clog*P*	IC_{50} (μM)
22[e]	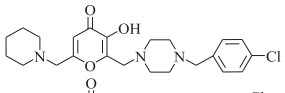	$C_{23}H_{30}ClN_3O_3$ 431.96	80	165–6	3.371	746
23[e]	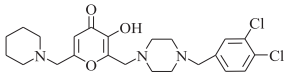	$C_{23}H_{29}Cl_2N_3O_3$ 466.40	32	151–2	3.964	204.1
24	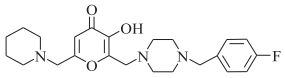	$C_{23}H_{30}FN_3O_3$ 401.47	60	159–60	2.801	232.3
25	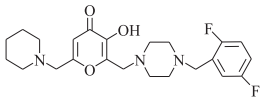	$C_{23}H_{29}F_2N_3O_3$ 433.49	54	102–4	2.944	> 2000
26	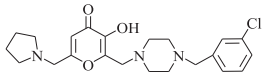	$C_{22}H_{28}ClN_3O_3$ 417.93	44	134–5	2.812	588.2
27[e]	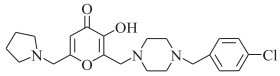	$C_{22}H_{28}ClN_3O_3$ 417.93	68	168–9	2.812	[**]nd
28[e]	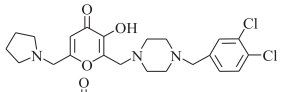	$C_{22}H_{27}Cl_2N_3O_3$ 452.37	20	143–4	3.405	94.1
29	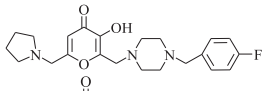	$C_{22}H_{28}FN_3O_3$ 401.47	20	147–9	2.242	225.5
30	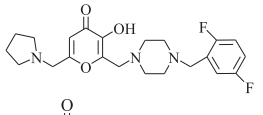	$C_{22}H_{27}F_2N_3O_3$ 419.46	55	108–10	2.385	1616
ALM	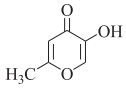	$C_6H_6O_3$ 126.11	63	152–3	0.15	411.6
CKA	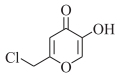	$C_6H_5ClO_3$ 160.56	76	166–7	0.21	413.7
KA	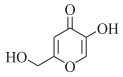	$C_6H_6O_4$ 142.11	–	152	−1.39	418.2

a:[19]; b:[16]; c:[15]; d:[10]; e[18].
* Decomposed.
** nd: not determined.
*** CAS registry number: 1324058-46-9.

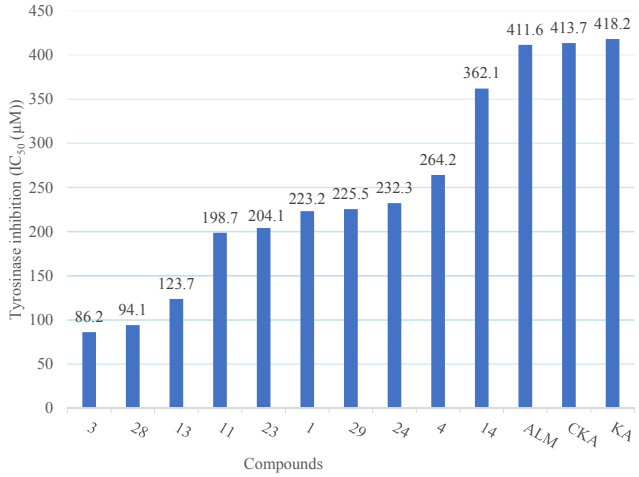

Scheme 2. IC_{50} values of the most active compounds (μM).

As shown in Fig. 1, each tropolone and KA bind very differently in tyrosinase crystals. This surprising observation was consistent with the literature. Also, there is a heterogeneity at the conformations of bivalent ions and zinc ions bind to protein at different locations. However, the mechanism underlying the coordination of KA in tyrosinase enzyme and interactions between KA and copper ions hasn't been fully clarified [25,26]. *Homo sapiens* tyrosinase protein TYRP1 was published in 2017 which has been detected in complex with zinc ion rather than copper ion. KA bound form of *Homo sapiens* tyrosinase protein showed that no coordination exists between KA and zinc ion [27].

In the crystal structure of tyrosine-tropolone complex, tropolone's seven-member aromatic ring makes sigma-pi contacts with Val283 and water molecule coordinated in the binding site doesn't have any interactions with protein. According to Ismaya et al. [22]. tropolone molecule does not bind to *A. bisporus* tyrosinase protein very specifically as the binding mode of tropolone differs for the four H units of tetramer. Furthermore, it has been stated that active site cavity of *A. bisporus* tyrosinase protein was large enough for more bulky substrates. Another research group revealed out that reversible tyrosinase inhibitor tropolone binds in the binding site without any conformational changes of the tyrosinase protein by building a pre-Michealis complex with deoxytyrosinase. Tropolone molecule doesn't make any interactions with water molecules or copper ions in the binding site [25]. Therefore, in this study, docking calculations were run in light of aforementioned literature.

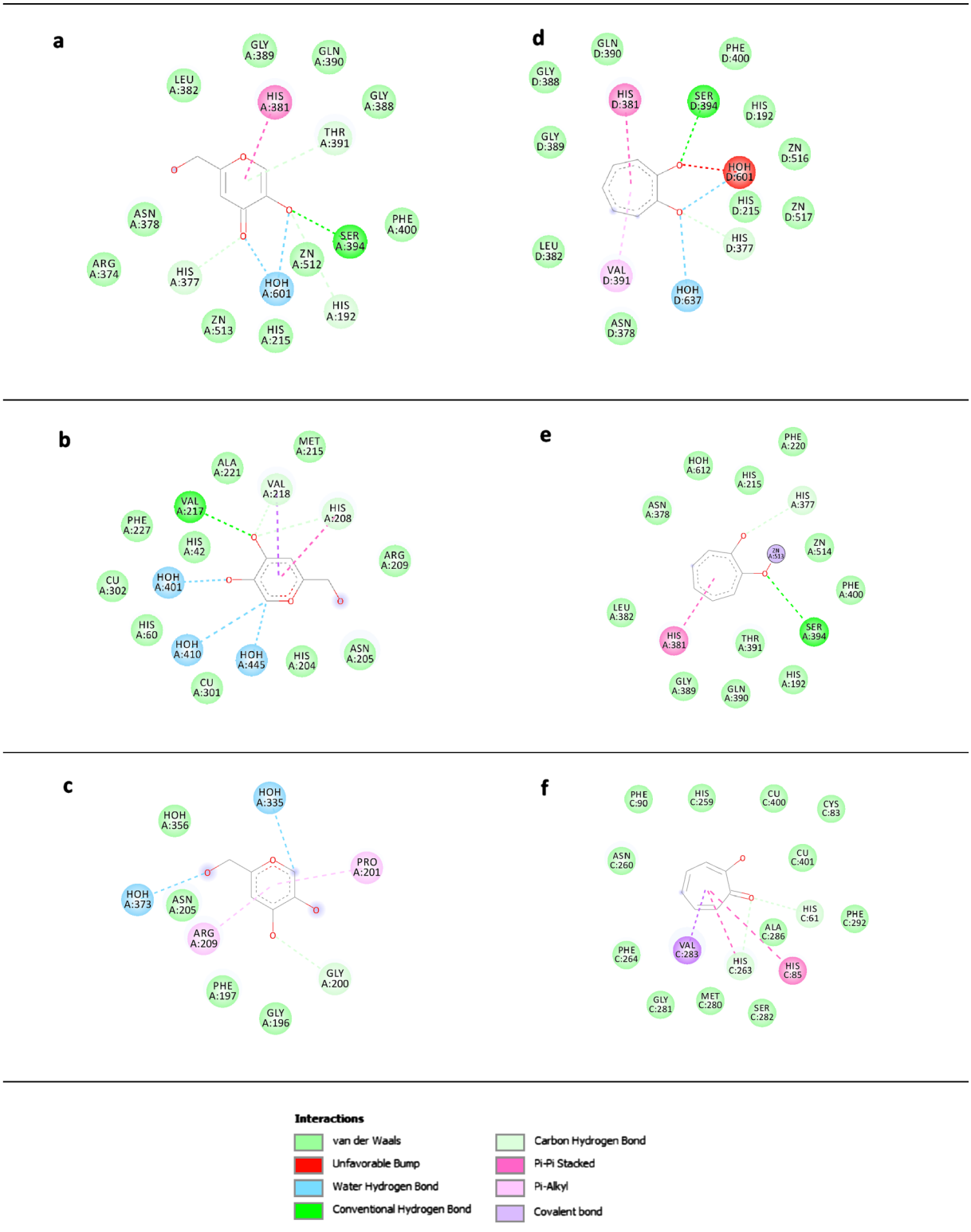

Fig. 1. Interactions between tyrosinase enzymes derived from different organisms and ligands as KA and tropolone. **a.** *H. sapiens* TYR with KOJ, PDB ID: 5M8M; **b.** *B. megaterium* TYR with KOJ PDB ID: 5I38; **c.** *B. megaterium* TYR with KOJ, PDB ID: 3NQ1; **d.** *H. sapiens* TYR with tropolone, PDB ID: 5M8T; **e.** *H. sapiens* TYR with tropolone, PDB ID: 5M8O; **f.** *A. bisporus* TYR with tropolone PDB ID: 2Y9X.

Regarding molecular modelling studies of the compounds, first but not least, no numerical correlation was found between binding affinities obtained from docking calculations and IC_{50} values of the all synthesized compounds. It was observed that binding modes of the compounds, possessing better antityrosinase activity, **1–5** significantly differs from the other compounds in the presence of copper ion. While Fig. 2 shows compounds **1–5** in the binding site, Fig. 3 demonstrates the interactions between the most active compound **3** and *A. bisporus*

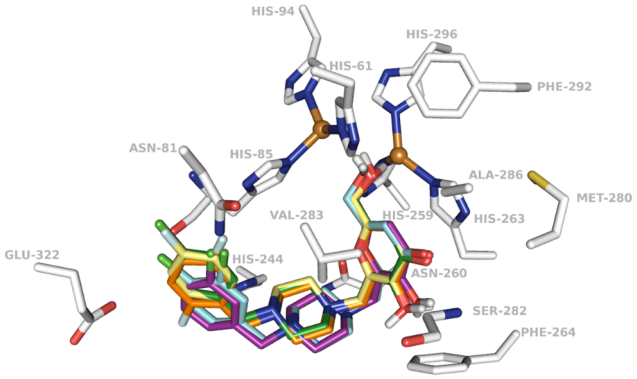

Fig. 2. Superposition of compounds **1–5** in tyrosinaze enzyme binding site.

tyrosinase enzyme.

According to the predicted conformation of compound **3** in the enzyme binding site, hydroxymethyl group provides a metal complex with copper ions and enzyme. His61, His85, His94, His259, His263 and His296 residues prominently support this complex. Chlorine substitution to phenyl ring makes a weak hydrogen bond with Asn81. The 4th-position oxygen atom of pyranone ring makes hydrogen bond interaction with Ser282. What is more, pi-pi stacked interactions between compound **3** and His263 were observed. Van der Waals contacts were detected between compound **3** and His61, Phe90, His244, His259, Met280, Gly281, Glu322, Phe292 and His296 amino acid residues. Pi-sigma contacts with Val283 as well as pi-alkyl contact with His85 and Val283 were obtained after docking of compound **3** to tyrosinase enzyme binding site. As a result, interactions especially the interaction between hydroxylmethyl group of compound **3** and copper ions explain the inhibitory activity of compound **3**. Amino acid residues which were found to play important role in inhibitory activity according to docking results comply with the literature [26].

Docking assays has shown that hydroxymethyl moiety at 6th-position of pyranone ring is important for binding to one of the copper ions of the active site of the mushroom tyrosinase providing a metal complex. Additionally, 3-chloro substituent of the benzyl group is of great potential as chlorine atom makes conventional hydrogen bond interacting with the enzyme.

Importance of hydroxymethyl substituent at the 6th-position of pyranone ring was mentioned above. From the molecular point of view, it is obvious that bulky substituted benzyl moiety addition to KA results in different binding conformation of KA derivatives. Fig. 2 shows possible binding conformation of the synthesized KA derivative compounds **1–5** possessing hydroxymethyl substituent at the 6th-position in the binding site of tyrosinase enzyme. Hydroxymethyl substituent is important to make complex with copper ion. Antityrosinase inhibitory activity results indicates that chlorine substution at the 3rd-position of the phenyl ring significantly enhances the activity. Docking results

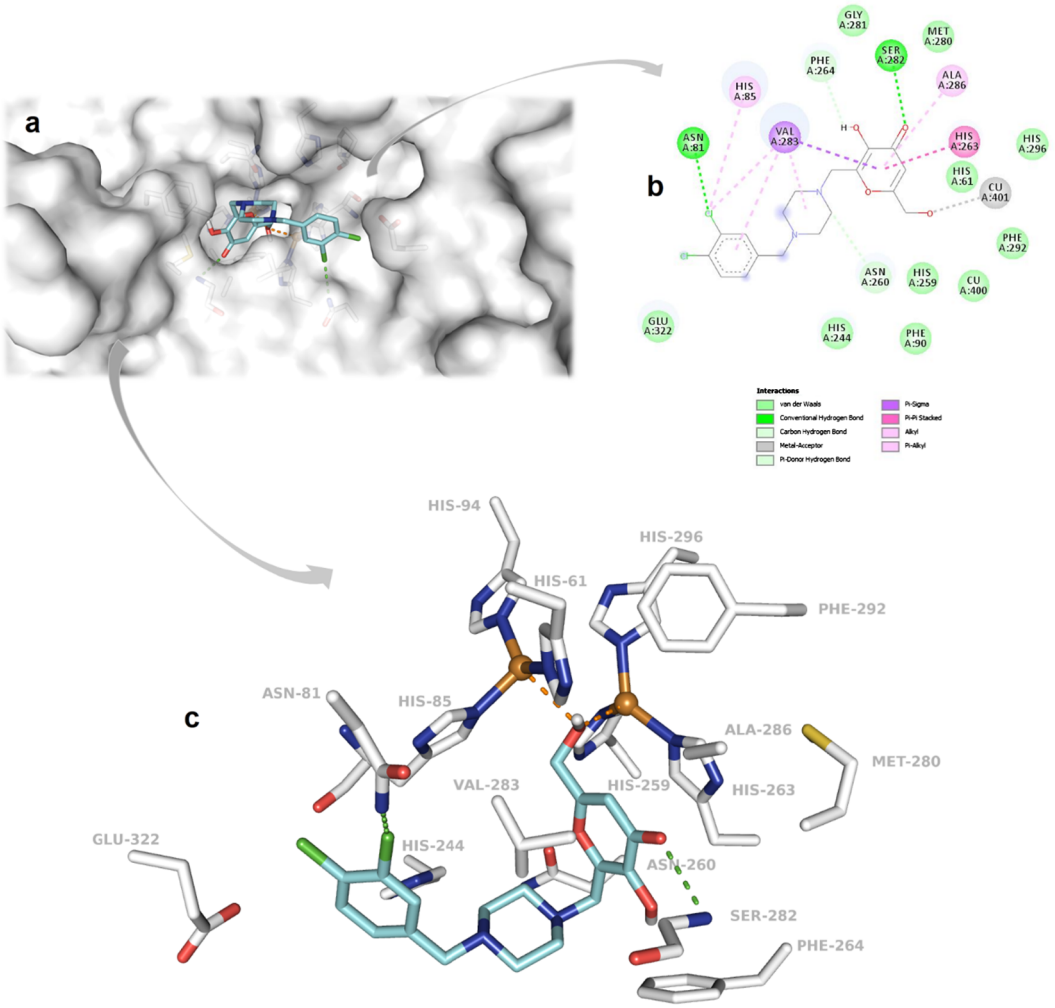

Fig. 3. Interactions between compound **3** and tyrosinase enzyme. **a.** Docked conformation of compound **3** in the binding pocket of *A. bisporus* TYR. **b.** 2D map stating the interactions between compound **3** and *A. bisporus* TYR. **c.** 3D map stating the interactions between compound **3** and *A. bisporus* TYR. Compound **3** is shown as cyan sticks and copper ions are show as brown spheres. Hydrogen bonds are depicted as green dashes while metal interactions are presented as orange dashes.

Table 2
Binding energies and IC_{50} values of the compounds **1–5.**

Compound	Binding energy (ΔG)	IC_{50} (μM)
1	−7.5	223.2
2	−7.8	710.0
3	−7.9	86.2
4	−7.8	264.2
5	−7.7	1564.0
Kojic acid	−5.5	418.2

provide consistent results with antityrosinase activity since it was shown that 3-chloro substituent of the benzyl group is also important as chlorine atom makes conventional hydrogen bond with Asn81. These finding explain the activity of the most active compounds **1** and **3** possessing IC_{50} values of 223.2 and 86.2 μM, respectively. In addition, phenyl ring interacts with His85 making pi-pi stacking contacts. In the presence of flourine atom at the 4th-position, electronegativity of phenyl ring increases and antityrosinase activity raises. Flourine substitution at 2nd- and 5th-position decreases the activity like chlorine substitution at 4th-position is inadequate to increase the inhibitory activity.

Among the compounds **1–5**, compound **3** which also has superior activity against tyrosinase enzyme showed the highest affinity to mushroom tyrosinase enzyme with −7.9 kcal/mol ΔG value. Obviously, hydrogen bond formation between the chlorine substitution of the phenyl ring and Asn81 residue helped to reduce binding energy of compound **3**. Moreover, as seen in Table 2, there is a big difference between the binding energy of kojic acid and synthesized compounds. Evaluating docking results, one should be aware of the importance of heavy atom contribution to the binding energy. Kojic acid is a much smaller compound than synthesized compounds **1–5** with the molecular formula of $C_6H_6O_4$. While heavy atom contribution explains the huge difference between binding energies of the compounds **1–5** and kojic acid, compounds **1–5** were found to be more active against tyrosinase enzyme compared to kojic acid as well.

3. Conclusion

In conclusion, a successful synthesis, characterization and biological evaluation and analysis of possible molecular interactions of KA derivatives as potent tyrosinase inhibitors have been described. The compounds **1–30** were synthesized starting from KA and various mono- or dihalogen-substituted benzylpiperazine derivatives employed by one pot Mannich reaction. Subsequently, compounds **16–30** were exposed to nucleophilic substitutions in basic medium with morpholine, piperidine or pyrrollidine rings. All the compounds **1–30** were screened for their potential activity against mushroom tyrosinase by a spectrophotometric method using L-DOPA as the substrate. The potential inhibitory activity of the compounds was also investigated *in silico* using molecular docking simulation method. Ten of the synthesized Mannich bases (compounds **3**, **28**, **13**, **11**, **23**, **1**, **29**, **24**, **4**, **14**) demonstrated higher inhibitory activities than KA which is both control agent and starting compound in this study. Molecular docking studies expressed a new point of view on the mechanism of chelation KA derivatives with copper ion of the tyrosinase enzyme. Contrary to expectations, instead of forming a bidentate copper-kojate dimer, the hydroxymethyl group at the 6th-position of the pyranone ring was found to be plausibly binding to copper ions on the active site of the enzyme. This explains the higher activities of the compounds **1**, **3** and **4** possessing hydroxymethyl substituent at the 6th-position supporting the mushroom assay results with docking studies. Docking studies and enzyme activity assays revealed that there is a significant relationship between structures and inhibitory activities of these compounds. In addition, 3,4-dichlorobenzyl moiety at the 2nd-position on KA skeleton (compounds **3**, **13**, **23**, **28**, and **29**) was found to be substantial for inhibitory activity. Especially, of the series, the most potent one compound **3**, inhibited tyrosinase enzyme activity with an IC_{50} value of 86.2 μM which is almost 5-fold higher than KA. It was clarified that this inhibitory activity may easily be used to reduce hyperpigmentation and the cytotoxicity generated by the compound is relatively low. According to the predicted conformation of compound **3** in the enzyme binding site, hydroxymethyl group provided a metal complex with copper ions and chlorine atom made conventional hydrogen bond interacting with the enzyme explaining the inhibitory activity. With this research and in the light of docking studies a new tyrosinase inhibition mechanism of Mannich bases based on the possible metal complex, H-bond and hydrophobic interactions between the side chain of Mannich bases is suggested. On the basis of the current study, it is concluded that the interaction between the inhibitor and the metal ion at the binding site has a crucial importance in the means of tyrosinase inhibition providing a new point of view in emphasizing the Mannich bases of KA as potent tyrosinase inhibitors. Thus, our present molecular docking studies could contribute to advance further and develop more potent tyrosinase inhibitors for the prevention of hyperpigmentation.

4. Experimental

4.1. Chemistry

All the chemicals used for the synthesis of the compounds were supplied by Merck (Darmstadt, Germany) and Aldrich Chemical Co. (Steinheim, Germany). Melting points were determined by a Thomas Hoover Capillary Melting Point Apparatus (Philadelphia, PA, USA) and presented as uncorrected. IR spectra were recorded on a Perkin Elmer FT-IR 420 System, Spectrum BX spectrometer. ^{1}H- and ^{13}C NMR spectra were obtained with a Varian Mercury 400 MHz spectrophotometer in deutorochloroform ($CDCl_3$) and dimethylsulphoxyde (DMSO-d_6). Tetramethylsilane (TMS) was used as an internal standard (chemical shift in δ, ppm). Mass analysis was carried out with a Micromass ZQ LC-MS with Masslynx Software Version 4.1 by using electrospray ionization (ESI+) method and HPLC with Waters Alliance by using C18 columns. Elementary analyses were performed with a Leco CHNS-932 analyzer (Leco, St. Joseph, MI, USA) in the Central Laboratory of Ankara University, Faculty of Pharmacy. The purity of the compounds was assessed by thin layer chromatography (TLC) on Kieselgel 60 F_{254} (Merck, Darmstadt, Germany) chromatoplates.

4.1.1. Synthesis of 3-hydroxy-6-chloromethyl/hydroxymethyl/methyl-2-substituted-4H-pyran-4-one derivatives (method I)

Secondary amine derivatives (substituted benzyl piperazine derivatives) and 37% formaline were dissolved in MeOH. KA, CKA or ALM was added to the solution and the mixture was stirred vigorously for 15 to 25 min. Resulting precipitate was collected by filtration and washed with cold MeOH. Crude products were recrystallized from the appropriate solvent.

4.1.1.1. 2-((4-(3-Chlorobenzyl)piperazin-1-yl)methyl)-3-hydroxy-6-(hydroxymethyl)-4H-pyran-4-one (compound 1). $C_{18}H_{21}ClN_2O_4$ (M.W.: 364.8 g/mol), yield: 91%; mp: 170–1 °C; clog P: 1.306; %CHN Found (Calculated): C 59.08 (59.26), H 5.76 (5.80), N 7.81 (7.68); IR ν (cm^{-1}): 3338 (O−H), 2976 (C−H (aliphatic)), 1653 (C=O), 1456 (C=C), 1088 (C−O); ^{1}H NMR (DMSO-d_6, 400 MHz) δ ppm: 2.37 (4H, brs, piperazine), 2.47–2.51 (4H, m, piperazine), 3.46 (2H, s, $-CH_2-$), 3.51 (2H, s, $-CH_2-$Ar), 4.29 (2H, s, $-CH_2$OH), 5.61 (1H, brs, $-CH_2OH$), 6.30 (1H, s, H^5), 7.23–7.36 (4H, m, Ar-*H*); ^{13}C NMR δ (DMSO-d_6, 100 MHz) 52.41, 53.56, 59.59, 61.08, 108.94, 126.85, 127.35, 128.34, 130.02, 132.90, 140.94, 143.5, 146.53, 167.58, 173.58; ESI-MS (*m/z*): 365 (100%, $(M)^+$), 367 $(M+H+2)^+$, 387 $(M+Na)^+$.

4.1.1.2. 2-((4-(4-Chlorobenzyl)piperazin-1-yl)methyl)-3-hydroxy-6-(hydroxymethyl)-4H-pyran-4-one (compound 2). $C_{18}H_{21}ClN_2O_4$ (M.W.: 364.8 g/mol), yield: 96%; mp: decomposed; clog P: 1.306; %CHN Found (Calculated): C 59.39 (59.26), H 5.76 (5.80), N 7.91 (7.68); IR ν (cm^{-1}): 1654 (C=O), 1456 (C=C), 1051 (C−O); ^{1}H NMR (DMSO-d_6, 400 MHz) δ ppm: 2.36–2.51 (8H; m; piperazine), 3.43 (2H; s; −CH_2−), 3.51 (2H; s; −CH_2−Ar), 4.28 (2H; s; −CH_2OH), 5.61 (1H; brs; −CH$_2$OH); 6.30 (1H; s; H^5), 7.30 (2H; d; J = 10.8 Hz; Ar-$H^{2''}$, $H^{6''}$), 7.36 (2H; d; J = 12.8 Hz; Ar-$H^{3''}$, $H^{5''}$); ^{13}C NMR δ (DMSO-d_6, 100 MHz) 52.30, 53.45, 59.48, 60.87, 108.83, 128, 130.25, 131.25, 137.12, 143.54, 146.42, 167.46, 173.47; ESI-MS (*m/z*): 365 (100%, $(M)^+$), 367 $(M+H+2)^+$, 387 $(M+Na)^+$.

4.1.1.3. 2-((4-(4-Fluorobenzyl)piperazin-1-yl)methyl)-3-hydroxy-6-(hydroxymethyl)-4H-pyran-4-one (compound 4). $C_{18}H_{21}FN_2O_4$ (M.W.: 348.4 g/mol), yield: 98%; mp: 187–8 °C; clog P: 0.736; %CHN Found (Calculated): C 62.14 (62.06), H 6.10 (6.08), N 8.11 (8.04); IR ν (cm^{-1}): 3245 (O−H), 1605 (C=O), 1454 (C=C), 1224 (C−O); ^{1}H NMR (DMSO-d_6, 400 MHz) δ ppm: 2.36 (4H, brs, piperazine), 2.47 (4H, brs, piperazine), 3.43 (2H, s, −CH_2−), 3.52 (2H, s, −CH_2−Ar), 4.31 (2H, s, −CH$_2$OH), 5.60 (1H, brs, −CH$_2$OH), 6.34 (1H, s, H^5), 7.12 (2H, t, J = 9.2 Hz, J = 8.4 Hz, Ar-$H^{3'}$. $H^{5'}$), 7.31 (2H, m, Ar-$H^{2'}$, $H^{6'}$); ^{13}C NMR δ (DMSO-d_6, 100 MHz) 52.36, 52.43, 53.58, 59.61, 61.07, 108.95, 114.73, 114.95, 130.55, 130.63, 134.30, 134.31, 143.69, 146.54, 160.03, 162.44, 167.60, 173.62; ESI-MS (*m/z*): 349 (100%, $(M+H)^+$); 350 $(M+2)^+$; 371 $(M+Na)^+$.

4.1.1.4. 2-((4-(2,5-Difluorobenzyl)piperazin-1-yl)methyl)-3-hydroxy-6-(hydroxymethyl)-4H-pyran-4-one (compound 5). $C_{18}H_{20}F_2N_2O_4$ (M.W.: 366.4 g/mol), yield: 72%; mp: 176–7 °C; clog P: 0.879; %CHN Found (Calculated): C 58.96 (59.01), H 5.41 (5.50), N 7.83 (7.65); IR ν (cm^{-1}): 3330 (O−H), 1617 (C=O), 1457 (C=C), 1179 (C−O); ^{1}H NMR (DMSO-d_6, 400 MHz) δ ppm: 2.41 (8H, brs, piperazine), 3.49 (2H, s, −CH_2−), 3.50 (2H, s, −CH_2−Ar), 4.29 (2H, s, −CH_2OH), 5.66 (1H, brs, −CH$_2$OH), 6.34 (1H, s, H^5), 7.09–7.23 (3H, brs, Ar-H); ESI-MS (*m/z*): 367 (100%, $(M+H)^+$); 389 $(M+Na)^+$.

4.1.1.5. 2-((4-(3-Chlorobenzyl)piperazin-1-yl)methyl)-6-(chloromethyl)-3-hydroxy-4H-pyran-4-one (compound 6). $C_{18}H_{20}Cl_2N_2O_3$ (M.W.: 382.90 g/mol) yield: 76%; mp: 147–8 °C; clog P: 2.906; %CHN Found (Calculated): C 56.18 (56.41), H 5.14 (5.26), N 7.30 (7.31); IR ν (cm^{-1}): 2943 (C−H), 1621 (C=O), 1455 (C=C), 1198 (C−O); ^{1}H NMR ($CDCl_3$, 400 MHz) δ ppm: 2.38 (4H; brs; piperazine-$H^{2'}$, $H^{6'}$), 2.50 (4H; brs; piperazine-$H^{3'}$, $H^{5'}$), 3.46 (2H; s; −CH_2−), 3.56 (2H; s; −CH_2−Ar), 4.65 (2H; s; ClCH_2-), 6.54 (1H; s; H^5), 7.23–7.36 (4H; m; Ar-H), 9.21 (1H; brs; −OH); ESI-MS (*m/z*): 383 (100%, $(M+H)^+$); 385 ($(M+H+2)^+$); 405 $(M+Na)^+$, 407 $(M+Na)^+$.

4.1.1.6. 2-((4-(3-Chlorobenzyl)piperazin-1-yl)methyl)-3-hydroxy-6-methyl-4H-pyran-4-one (compound 11). $C_{18}H_{21}ClN_2O_3$ (M.W.: 348.8 g/mol), yield: 63%; mp: 158–9 °C; clog P: 2.843; ESI-MS (*m/z*): 160 (100%), 349 $(M+H)^+$); 371 $(M+Na)^+$. *Commercially sold, CAS registry number: 1324058–46-9.*

4.1.1.7. 2-((4-(4-Fluorobenzyl)piperazin-1-yl)methyl)-3-hydroxy-6-methyl-4H-pyran-4-one (compound 14). $C_{18}H_{21}FN_2O_3$ (M.W.: 332.4 g/mol), yield: 66%; mp: 168–70 °C; clog P: 2.273; %CHN Found (Calculated): C 65.00 (65.05), H 6.66 (6.37), N 8.53 (8.43); IR ν (cm^{-1}): 2944, 2816 (C−H (aliphatic)), 1622 (C=O), 1511, 1456 (C=C), 1147 (C−O). ^{1}H NMR ($CDCl_3$, 400 MHz) δ ppm: 2.25 (3H, s, −CH_3), 2.46 (4H, brs, piperazine), 2.60 (4H, brs, piperazine), 3.44 (2H, s, pyrane-CH_2-piperazine), 3.62 (2H, s, −CH_2−Ar), 6.16 (1H, t, pyrane-H^5), 6.95 (2H, t, Ar-$H^{3',5'}$). 7.22 (2H, m, Ar-$H^{2',6'}$); ^{13}C NMR δ ($CDCl_3$, 100 MHz) 20.13, 52.81, 55.23, 62.23, 111.31, 122.82, 123.96, 125.60, 128.23, 128.67, 129.18, 130.11, 130.43, 130.75, 131.07, 132.32, 139.10, 143.51, 145.22, 165.22, 173.95; ESI-MS (*m/z*): 332 (100%, $(M)^+$).

4.1.1.8. 2-((4-(2,5-Difluorobenzyl)piperazin-1-yl)methyl)-3-hydroxy-6-methyl-4H-pyran-4-one (compound 15). $C_{18}H_{20}F_2N_2O_3$ (M.W.: 350.4 g/mol), yield: 70%; mp: 163–5 °C; clog P: 2.416; %CHN Found (Calculated): C 61.58 (61.71), H 5.91 (5.75), N 8.20 (8.00); IR ν (cm^{-1}): 2812 (C−H (aliphatic)), 1641 (C=O), 1460 (C=C), 987 (C−O); ^{1}H NMR (DMSO-d_6, 400 MHz) δ ppm: 2.22 (3H, s, −CH_3), 2.43 (4H, brs, piperazine), 2.48 (4H, t, piperazine), 3.47 (2H, s, pyrane-CH_2-piperazine), 3.48 (2H, s, −CH_2−Ar), 6.18 (1H, s, pyrane-H^5), 7.09–7.22 (3H, m, Ar-H); ESI-MS (*m/z*): 351 (100%, $(M)^+$), 353 $(M+2)^+$.

4.1.2. Synthesis of 2-((4-(substituted benzyl)piperazine-1-yl)methyl)-3-hydroxy-6-(morpholinyl/piperidinyl/pyrrolidinylmethyl)-4H-pyran-4-one derivatives (method II)

Morpholine, piperidine or pyrrolidine were dissolved in dimethylformamide (DMF). Mannich base and K_2CO_3 was added to the solution in ice bath, respectively. The reaction mixture was stirred for 36 h. The progress of the reaction was followed by TLC using chloroform:methanol (7:3) as solvent. After the completion of the reaction, the mixture was poured into iced water and extracted using dichloromethane. The organic phase was evaporated to dryness which were further purified by recrystallization in ethyl acetate or ethyl acetate/petroleum ether.

4.1.2.1. 2-((4-(3-Chlorobenzyl)piperazin-1-yl)methyl)-3-hydroxy-6-(morpholinomethyl)-4H-pyran-4-one (compound 16). $C_{22}H_{28}ClN_3O_4$ (M.W.: 433.9 g/mol), yield: 13%, mp: 137–8 °C, clog P: 2.091; %CHN Found (Calculated): C 60.33 (60.89), H 6.83 (6.50), N 9.80 (9.68); IR ν (cm^{-1}): 2951, 2808 (C−H (aliphatic)), 1618 (C=O), 1456 (C=C), 867 (C−O); ^{1}H NMR ($CDCl_3$, 400 MHz) δ ppm: 2.49–2.52 (8H, t, piperazine-H), 2.62 (4H, brs, morpholine-CH_2-N), 3.37 (2H, s, morpholine-CH_2-pyrane), 3.47 (2H, s, pyrane-CH_2-piperazine), 3.66 (2H, s, −CH_2−Ar), 3.70 (4H, t, morpholine-CH_2-O), 6.46 (1H, s, pyrane-H^5), 7.15–7.25 (3H, m, Ar-H), 7.30 (1H, s, Ar-H); ^{13}C NMR δ ($CDCl_3$, 100 MHz) 52.76, 52.86, 53.47, 55.37, 59.78, 62.16, 66.80, 111.68, 127.13, 127.31, 128.97, 129.49, 134.19, 140.11, 143.94, 145.44, 164.49, 173.83; ESI-MS (*m/z*): 218 (100%), 434 $(M)^+$, 436 $(M+2)^+$.

4.1.2.2. 2-((4-(3,4-dichlorobenzyl)piperazin-1-yl)methyl)-3-hydroxy-6-(morpholinomethyl) −4H-pyran-4-one (compound 18). $C_{22}H_{28}Cl_2N_3O_4$ (M.W.: 468.4 g/mol), yield: 12%, mp: 142–4 °C, clog P: 2.684; %CHN Found (Calculated): C 55.79 (56.42), H 5.93 (5.81), N 9.27 (8.97); IR ν (cm^{-1}): 2956, 2803 (C−H (aliphatic)), 1618 (C=O), 1457 (C=C), 1003 (C−O); ^{1}H NMR ($CDCl_3$, 400 MHz) δ ppm: 2.53 (8H, t, J = 4.2, piperazine-H), 2.64 (4H, brs, morpholine-CH_2-N), 3.39 (2H, s, morpholine-CH_2-pyrane), 3.45 (2H, s, pyrane-CH_2-piperazine), 3.68 (2H, s, −CH_2−Ar), 3.72 (4H, t, J = 4.6 Hz, morpholine-CH_2-O), 6.48 (1H, s, pyrane-H^5), 7.14 (1H, dd, J = 8.4 Hz, J = 2 Hz, Ar-$H^{6'}$), 7.36 (1H, d, J = 8.0 Hz Ar-$H^{5'}$), 7.42 (1H, d, J = 2 Hz, Ar-$H^{2'}$); ^{13}C NMR δ ($CDCl_3$, 100 MHz) 52.76, 52.83, 53.47, 55.24, 59.74, 61.51, 66.80, 111.64, 128.24, 130.18, 130.70, 130.99, 132.33, 138.46, 143.94, 145.51, 164.56, 173.84; ESI-MS (*m/z*): 234 (100%), 468 $(M)^+$, 470 $(M+2)^+$.

4.1.2.3. 2-((4-(4-Fluorobenzyl)piperazin-1-yl)methyl)-3-hydroxy-6-(morpholinomethyl)-4H-pyran-4-one (compound 19). $C_{22}H_{28}FN_3O_4$ (M.W.: 417.5 g/mol), yield: 45%, mp: 156–7 °C, clog P: 1.521; %CHN Found (Calculated): C 63.15 (63.29), H 6.56 (6.76), N 10.16 (10.07); IR ν (cm^{-1}): 2950 (C−H (aliphatic)), 1618 (C=O), 1457 (C=C), 1117 (C−O). ^{1}H NMR ($CDCl_3$, 400 MHz) δ ppm: 2.50 (8H, t, piperazine-H), 2.61 (4H, brs, morpholine-CH_2-N), 3.36 (2H, s, morpholine-CH_2-pyrane), 3.45 (2H, s, pyrane-CH_2-piperazine), 3.65 (2H, s, −CH_2-Ar), 3.69 (4H, t, morpholine-CH_2-O), 6.45 (1H, s, pyrane-H^5), 6.97 (2H, t, Ar-$H^{3',5'}$), 7.24 (2H, t, Ar-$H^{2',6'}$); ^{13}C NMR δ ($CDCl_3$, 100 MHz) 52.67, 52.87, 53.46, 55.35, 59.73, 61.99, 66.79, 111.70, 114.91, 115.12, 130.56, 133.53, 143.97, 145.53, 160.79, 163.22, 164.45, 173.85; ESI-MS (*m/z*) 418 (100%, $(M+H)^+$).

4.1.2.4. 2-((4-(2,5-Difluorobenzyl)piperazin-1-yl)methyl)-3-hydroxy-6-(morpholinomethyl)-4H-pyran-4-one (compound 20). $C_{22}H_{27}F_2N_3O_4$ (M.W.: 435.5 g/mol), yield: 28%, mp: 107–8 °C, clog P: 1.664; %CHN ($C_{22}H_{27}F_2N_3O_4.2CH_3OH$) Found (Calculated): C 57.58 (57.70), H 6.24 (7.06), N 9.29 (8.41); IR ν (cm^{-1}): 2816 (C—H (aliphatic)), 1632 (C=O), 1496, 1448 (C=C), 998 (C—O); ^{1}H NMR ($CDCl_3$, 400 MHz) δ ppm: 2.50–2.53 (8H, brs, piperazine-*H*), 2.62 (4H, s, morpholine-C*H*$_2$-N), 3.37 (2H, s, morpholine-C*H*$_2$-pyrane), 3.54 (2H, s, pyrane-C*H*$_2$-piperazine), 3.65 (2H, s, −C*H*$_2$-Ar), 3.70 (4H, t, morpholine-C*H*$_2$-O), 6.44 (1H, s, pyrane-*H*^{5}), 6.86–7.1 (3H, m, Ar-*H*), 7.26 (1H, brs, −O*H*); ^{13}C NMR δ ($CDCl_3$, 100 MHz) 52.48, 52.87, 53.48, 54.66, 55.07, 59.86, 66.69, 111.80, 144.95, 145.53, 155.96, 157.42, 158.36, 159.80, 164.30, 173.84; ESI-MS (*m/z*) 218 (100%), 436 $(M+H)^+$, 458 $(M+Na)^+$.

4.1.2.5. 2-((4-(3-Chlorobenzyl)piperazin-1-yl)methyl)-3-hydroxy-6-(piperidin-1-ylmethyl)-4H-pyran-4-one (compound 21). $C_{23}H_{30}ClN_3O_4$ (M.W.: 432.0 g/mol), yield: 58%, mp: 145–7 °C, clog P: 3.371; %CHN Found (Calculated): C 63.56 (63.95), H 6.92 (7.00), N 9.77 (9.73); IR ν (cm^{-1}): 2937, 2786 (C—H (aliphatic)), 1619 (C=O), 1455 (C=C); ^{1}H NMR ($CDCl_3$, 400 MHz) δ ppm: 1.43–1.44 (2H, m, piperidine^4-*H*), 1.56–1.61 (4H, m, piperidine^{3,5}-*H*), 2.43–2.45 (4H, t, *J* = 5.2 Hz, piperidine^{2,6}-*H*), 2.65 (8H, brs, piperazine), 3.34 (2H, s, piperidine-C*H*$_2$-pyrane), 3.49 (2H, s, pyrane-C*H*$_2$-piperazine), 3.68 (2H, s, –C*H*$_2$-Ar), 6.46 (1H, s, pyrane-*H*^{5}), 7.18–7.27 (4H, m, Ar-*H*), 7.32 (1H, s, Ar-*H*); ^{13}C NMR δ ($CDCl_3$, 100 MHz) 23.91, 25.87, 52.75, 52.81, 54.55, 55.36, 60.25, 62.13, 111.50, 127.15, 127.33, 129.45, 134.20, 140.04, 143.81, 145.14; ESI-MS (*m/z*) 217 (100%), 432 $(M)^+$.

4.1.2.6. 2-((4-(4-Fluorobenzyl)piperazin-1-yl)methyl)-3-hydroxy-6-(piperidin-1-ylmethyl)-4H-pyran-4-one (compound 24). $C_{23}H_{30}FN_3O_3$ (M.W.: 401.5 g/mol), yield: 60%, mp: 159–60 °C, clog P: 2.801; %CHN Found (Calculated): C 66.06 (65.82), H 7.04 (7.03), N 10.26 (10.47); IR ν (cm^{-1}): 2938, 2808 (C—H (aliphatic)), 1623 (C=O), 1496 (C=C). ^{1}H NMR ($CDCl_3$, 400 MHz) δ ppm: 1.40–1.43 (2H, m, piperidine^4-*H*), 1.54–1.60 (4H, m, piperidine^{3,5}-*H*), 2.42 (4H, t, *J* = 5.2 Hz, piperidine^{2,6}-*H*), 2.62 (8H, brs, piperazine), 3.24 (2H, s, piperidine-C*H*$_2$-pyrane), 3.47 (2H, s, pyrane-C*H*$_2$-piperazine), 3.65 (2H, s, −C*H*$_2$−Ar), 6.44 (1H, s, pyrane-*H*^{5}), 6.45–6.49 (2H, m, Ar-*H*$^{3',5'}$), 7.23–7.27 (2H, m, Ar-*H*$^{2',6'}$); ^{13}C NMR δ ($CDCl_3$, 100 MHz) 23.89, 25.83, 52.65, 52.82, 54.55, 55.27, 60.27, 61.94, 111.57, 114.92, 115.13, 130.61, 143.86, 145.29, 160.81, 163.24, 165.46, 173.93; ESI-MS (*m/z*) 233 (100%), 466 $(M)^+$, 468 $(M+2)^+$.

4.1.2.7. 2-((4-(2,5-Difluorobenzyl)piperazin-1-yl)methyl)-3-hydroxy-6-(piperidin-1-yl-methyl)-4H-pyran-4-one (compound 25). $C_{23}H_{29}F_2N_3O_3.1/2CH_3OH$ (M.W.: 433.5 g/mol), yield: 54%, mp: 102–4 °C, clog P: 2.994; %CHN Found (Calculated): C 62.79 (62.79), H 7.01 (6.95), N 9.62 (9.35); IR ν (cm^{-1}): 3334 (O—H), 2941, 2816 (C—H (aliphatic)), 1632 (C=O), 1496, 1447 (C=C); ^{1}H NMR ($CDCl_3$, 400 MHz) δ ppm: 1.43–1.44 (2H, m, piperidine^4-*H*), 1.55–1.61 (4H, m, piperidine^{3,5}-*H*), 2.44 (4H, t, *J* = 5.2 Hz, piperidine-C*H*$_2$-N), 2.55–2.65 (8H, brs, piperazine), 3.35 (2H, s, piperidine-C*H*$_2$-pyrane), 3.56 (2H, s, pyrane-C*H*$_2$-piperazine), 3.67 (2H, s, −C*H*$_2$−Ar), 6.46 (1H, s, pyrane-*H*^{5}), 6.88–7.12 (3H, m, Ar-*H*), 7.27 (1H, brs, −O*H*); ^{13}C NMR δ ($CDCl_3$, 100 MHz) 23.89, 25.87, 52.56, 52.80, 54.53, 54.67, 55.20, 60.23, 111.45, 143.82, 145.28, 155.96, 157.42, 158.37, 159.82, 165.61,173.92; ESI-MS (*m/z*) 218 (100%), 435 $(M+H)^+$, 457 $(M+Na)^+$.

4.1.2.8. 2-((4-(3-Chlorobenzyl)piperazin-1-yl)methyl)-3-hydroxy-6-(pyrrolidin-1-ylmethyl)-4H-pyran-4-one (compound 26). $C_{22}H_{28}ClN_3O_3$ (M.W.: 417.9 g/mol), yield: 44%, mp: 134–5 °C, clog P: 2.812; %CHN Found (Calculated): C 62.46 (63.22), H 6.80 (6.75), N 10.08 (10.05); IR ν (cm^{-1}): 2943, 2809 (C—H (aliphatic)), 1626 (C=O), 1497, 1454 (C=C), 1006 (C—O). ^{1}H NMR ($CDCl_3$, 400 MHz) δ ppm: 1.79 (4H, brs, pyrrolidine^{3,4}-*H*), 2.49 (4H, brs, pyrrolidine ^{2,5}-*H*), 2.58 (4H, brs, piperazine), 2.63 (4H, brs, piperazine), 3.47 (2H, s, pyrrolidine-C*H*$_2$-pyrane), 3.49 (2H, s, pyrane-C*H*$_2$-piperazine), 3.66 (2H, s, −C*H*$_2$−Ar), 6.42 (1H, s, pyrane-*H*^{5}), 7.16–7.26 (4H, m, Ar-*H*), 7.31 (1H, s, Ar-*H*); ^{13}C NMR δ ($CDCl_3$, 100 MHz) 23.61, 52.76, 52.85, 54.14, 55.47, 57.07, 62.15, 111.44, 127.14, 127.30, 134.22, 140.12, 143.88, 145.19, 165.62, 173.98; ESI-MS (*m/z*) 210 (100%), 419 $(M+H)^+$.

4.1.2.9. 2-((4-(4-Fluorobenzyl)piperazin-1-yl)methyl)-3-hydroxy-6-(pyrrolidin-1-ylmethyl)-4H-pyran-4-one (compound 29). $C_{22}H_{28}FN_3O_3$ (M.W.: 401.5 g/mol), yield: 20%, mp: 147–9 °C, clog P: 2.242. %CHN Found (Calculated): C 65.58 (65.82), H 7.44 (7.03), N 10.54 (10.47); IR ν (cm^{-1}): 2957, 2875, 2812 (C—H (aliphatic)), 1624 (C=O), 1447 (C=C), 1007 (C—O); ^{1}H NMR ($CDCl_3$, 400 MHz) δ ppm: 1.77–1.80 (4H, m, pyrrolidine ^{3,4}-*H*), 2.48 (4H, brs, pyrrolidine ^{2,5}-*H*), 2.56–2.63 (8H, m, piperazine), 3.46 (2H, s, pyrrolidine-C*H*$_2$-pyrane), 3.49 (2H, s, pyrane-C*H*$_2$-piperazine), 3.65 (2H, s, −C*H*$_2$−Ar), 6.41 (1H, s, pyrane-*H*^{5}), 6.96 (2H, t, Ar-*H*$^{3',5'}$), 7.23–7.27 (2H, m, Ar-*H*$^{2',6'}$) ^{13}C NMR δ ($CDCl_3$, 100 MHz) 23.59, 52.62, 52.80, 54.13, 55.35, 57.09, 61.92, 111.47, 114.92, 115.14, 130.65, 133.38, 143.93, 145.28, 160.81, 163.25, 165.51, 174.02; ESI-MS (*m/z*) 402 (100%, $(M+H)^+$).

4.1.2.10. 2-((4-(2,5-Difluorobenzyl)piperazin-1-yl)methyl)-3-hydroxy-6-(pyrrolidin-1-yl- methyl)-4H-pyran-4-one (compound 30). $C_{22}H_{27}F_2N_3O_3$ (M.W.: 419.5 g/mol), yield: 55%, mp: 108–10 °C, clog P: 2.385; %CHN ($C_{22}H_{27}F_2N_3O_3{\cdot}H_2O$) Found (Calculated): C 60.34 (60.40), H 6.72 (6.68), N 9.73 (9.61); IR ν (cm^{-1}): 2813 (C—H (aliphatic)), 1632 (C=O), 1496 (C=C), 1000 (C—O). ^{1}H NMR ($CDCl_3$, 400 MHz) δ ppm: 1.66–1.69 (4H, m, pyrrolidine^{3,4}-*H*), 2.40 (4H, brs, pyrrolidine^{2,5}-*H*), 2.47–2.51 (8H, brs, piperazine), 3.47 (2H, s, pyrrolidine-C*H*$_2$-pyrane), 3.50 (2H, s, pyran-C*H*$_2$-piperazine), 3.52 (2H, s, −C*H*$_2$−Ar), 6.31 (1H, s, pyrane-*H*^{5}), 7.09–7.23 (3H, m, Ar-*H*). ^{13}C NMR δ ($CDCl_3$, 100 MHz) 23.22, 52.26, 52.29, 53.22, 53.38, 54.01, 55.84, 111.17, 115.06, 115.15, 115.30, 115.39, 116.41, 116.50, 116.66, 116.75, 116.97, 117.02, 117.21, 117.26, 143.70, 146.82, 15.57, 155.59, 156.84, 156.86, 157.96, 157.98, 159.24, 164.97, 173.53; ESI-MS (*m/z*) 420 (100%, $(M+H)^+$).

4.2. Mushroom tyrosinase assay

The enzymatic activity of mushroom tyrosinase is substrate dependent. To investigate the enzyme inhibition of mushroom tyrosinase the oxidation rate of L-DOPA was measured spectrophotometrically [35] where KA was used as a standart compound. In 96 well plates 100 µl of 50 mM phosphate buffer (pH 6.8), 10 µl of inhibitor/DMSO, 10 µl of enzyme (Sigma, T3824) in 50 mM pH 6.5 phosphate buffer was prepared. The wells which contain dimethyl sulfoxide (DMSO) instead of the compounds were considered as control groups. KA, which is known to inhibit tyrosinase, was handled as positive control. The mixture was preincubated for 10 min at 37 °C and the reaction was initiated with 30 µl of 5 mM L-DOPA (Sigma, D9628) addition. At the end of 20 min incubation, absorbance values of the samples at 492 nm were recorded using ELISA Plate Reader (BioTek PowerWawe). The % inhibiton was calculated by substracting the values obtained by DMSO addition. Increasing concentrations of each compound (8–2000 µM) were tested in triplicates and the IC_{50} values were assessed by constructing a non-linear regression curve using GraphPad Prism 5.03. The IC_{50} values of mushroom tyrosinase inhibition for each compound was presented in Table 1.

% Inhibition values were calculated compared to the control by using the formula below;

$$\% \text{ Inhibition} = (A - B)/ A \times 100$$

A: Absorbance of DMSO at 492 nm

B: Absorbance of the samples at 492 nm

GraphPad Prism 5.03 software was used to determine IC_{50} values

and standard deviations. All of the measurements were carried out to be triplicate (n = 3) [28].

4.3. Molecular docking assay

In protein data bank, 55 different tyrosinase enzyme crystal structures are accessible which were derived from *Homo sapiens*, *Streptomyces castaneoglobisporus*, *Bacillus megaterium* or *Agaricus bisporus*. They are also crystallized with different substrates. PDB ID codes and ligands inside of the tyrosinase enzymes are presented in Supplementary Data. *A. bisporus* tyrosinase enzyme was selected for docking calculations derived from Protein Data Bank (PDB ID: 2X9Y) since mushroom tyrosinase enzyme was used to test antityrosinase activity of the compounds. Biovia Discovery Studio Visualizer and MGLTools software were used to prepare data before docking. Holmium atom was removed from the protein for calculations. Polar hydrogen atoms and were added to protein. 3D structures of ligands were also prepared. Gasteiger charges were assigned to the ligands and the receptor. Protonation states of histidine amino acid residues were determined. Histidines apart from His61, His85, His94, His259, His263 and His296 were prepared as charged forms while mentioned histidine residues which bind to copper ions were assigned as 0HD1 forms. Ligands were prepeared with Biovia Discovery Studio Visualizer and MGLTools. Autodock Vina software was used for docking calculations. Binding modes of the ligands were evaluated with PMV and PyMOL.

Conflict of interest

None of the authors of the above manuscript has declared any conflict of interest which may arise from being named as an author on the manuscript.

Acknowledgements

This study was partially supported by The Scientific and Technological Research Council of Turkey (TUBITAK Project number: SBAG 315S067 and 111S311) and Hacettepe University Scientific Research Projects Coordination Unit (THD-2015-7392 and 09D01301002-4756) as a part of PhD thesis.

Appendix A. Supplementary material

Supplementary data to this article can be found online at https://doi.org/10.1016/j.bioorg.2019.102950.

References

[1] T.-S. Chang, An updated review of tyrosinase inhibitors, Int. J. Mol. Sci. 10 (2009) 2440–2475.
[2] J.-M. Noh, S.-Y. Kwak, H.-S. Seo, J.-H. Seo, B.-G. Kim, Y.-S. Lee, Kojic acid–amino acid conjugates as tyrosinase inhibitors, Bioorg. Med. Chem. Lett. 19 (2009) 5586–5589.
[3] H. Hamidian, S. Azizi, Synthesis of novel compounds containing morpholine and 5(4H)-oxazolone rings as potent tyrosinase inhibitors, Bioorg. Med. Chem. 23 (2015) 7089–7094.
[4] F. Azami, E. Tazikeh-Lemezki, M. Mahmood-Janlou, Kojic acid effect on the inhibitory potency of tyrosinase, J. Chem. Health Risks 7 (2017) 147–155.
[5] Z. Chen, D. Cai, D. Mou, Q. Yan, Y. Sun, W. Pan, et al., Design, synthesis and biological evaluation of hydroxy- or methoxy- substituted 5-benzylidene(thio)barbiturates as novel tyrosinase inhibitors, Bioorg. Med. Chem. 22 (2014) 3279–3284.
[6] M.T.H. Khan, Molecular design of tyrosinase inhibitors: A critical review of promising novel inhibitors from synthetic origins, Pure Appl. Chem. 79 (2007) 2277–2295.
[7] T. Raku, Y. Tokiwa, Regioselective synthesis of kojic acid esters by Bacillus subtilis protease, Biotechnol. Lett. 25 (2003) 969–974.
[8] H.S. Rho, S.M. Ahn, D.S. Yoo, M.K. Kim, D.H. Cho, J.Y. Cho, Kojyl thioether derivatives having both tyrosinase inhibitory and anti-inflammatory properties, Bioorg. Med. Chem. Lett. 20 (2010) 6569–6571.
[9] S.-Y. Kwak, J.-M. Noh, S.-H. Park, J.-W. Byun, H.-R. Choi, K.-C. Park, et al., Enhanced cell permeability of kojic acid–phenylalanine amide with metal complex, Bioorg. Med. Chem. Lett. 20 (2010) 738–741.
[10] B. Berk, D. Us, S. Öktem, Z.T. Kocagöz, B. Çağlayan, I.A. Kurnaz, et al., Molecular modeling and antimycobacterial studies of mannich bases: 5-Hydroxy-2-methyl-4*H*-pyran-4-ones, Turk. J. Chem. 35 (2011) 317–330.
[11] M.D. Aytemir, G. Karakaya, Kojic acid derivatives (Ed.: D. Ekinci), Medicinal Chemistry and Drug Design, InTech, Rijeka (2012), chapter 1.
[12] M.-J. Chen, C.-C. Hung, Y.-R. Chen, S.-T. Lai, C.-F. Chan, Novel synthetic kojic acid-methimazole derivatives inhibit mushroom tyrosinase and melanogenesis, J. Biosci. Bioeng. 122 (2016) 666–672.
[13] Y.-M. Chen, W.-C. Su, C. Li, Y. Shi, Q.-X. Chen, J. Zheng, D.-L. Tang, S.-M. Chen, Q. Wang, Anti-melanogenesis of novel kojic acid derivatives in B16F10 cells and zebrafish, Int. J. Biol. Macromol. 123 (2019) 723–731.
[14] M.D. Aytemir, B. Ozcelik, A study of cytotoxicity of novel chlorokojic acid derivatives with their antimicrobial and antiviral activities, Eur. J. Med. Chem. 45 (2010) 4089–4095.
[15] M.D. Aytemir, B. Ozcelik, G. Karakaya, Evaluation of bioactivities of chlorokojic acid derivatives against dermatophytes couplet with cytotoxicity, Bioorg. Med. Chem. Lett. 23 (2013) 3646–3649.
[16] G. Karakaya, M.D. Aytemir, B. Özçelik, Ü. Çalış, Design, synthesis and *in vivo/in vitro* screening of novel chlorokojic acid derivatives, J. Enz. Inh. Med. Chem. 28 (2013) 627–638.
[17] M.D. Aytemir, New approaches for tyrosinase inhibitors: Mannich bases of kojic acid derivatives, Med. Chem. 6 (2016) 8, https://doi.org/10.4172/2161-0444.C1.024.
[18] G. Karakaya, A. Ercan, S. Oncul, M.D. Aytemir, Synthesis and cytotoxic evaluation of kojic acid derivatives with inhibitory activity on melanogenesis in human melanoma cells, Anticancer Agents Med. Chem. 18 (2018) 2137–2148.
[19] M.D. Aytemir, B. Özçelik, İ. Orhan Erdoğan, G. Karakaya, F.S. Şenol, Kojic acid-derived mannich bases with biological effect [Turkish Patent: TR2015/07653-WO2016/209180, International Patent: PCT/TR2016/000070 - US 9,975,884 B2, May 22, 2018].
[20] S. Okombi, D. Rival, S. Bonnet, A.-M. Mariotte, E. Perrier, A. Boumendjel, Analogues of N-hydroxycinnamoylphenalkylamides as inhibitors of human melanocyte-tyrosinase, Bioorg. Med. Chem. Lett. 16 (2006) 2252–2255.
[21] Q.-X. Chen, I. Kubo, Kinetics of mushroom tyrosinase inhibition by quercetin, J. Agric. Food Chemi. 50 (2002) 4108–4112.
[22] W.T. Ismaya, H.J. Rozeboom, A. Weijn, J.J. Mes, F. Fusetti, H.J. Wichers, Crystal structure of Agaricus bisporus mushroom tyrosinase: identity of the tetramer subunits and interaction with tropolone, Biochemistry 50 (2011) 5477–5486.
[23] C. Ribeiro Lima, J.R.A. Silva, E.T.C. Cardoso, E.O. Silva, J. Lameira, J.L.M. Nascimento, et al., Combined kinetic studies and computational analysis on kojic acid analogs as tyrosinase inhibitors, Molecules 19 (2014) 9591–9605.
[24] A. Asadzadeh, H. Sirous, M. Pourfarzam, P. Yaghmaei, A. Fassihi, In vitro and in silico studies of the inhibitory effects of some novel kojic acid derivatives on tyrosinase enzyme, IJBMS 19 (2016) 132–144.
[25] M. Sendovski, M. Kanteev, V.S. Ben-Yosef, N. Adir, A. Fishman, First structures of an active bacterial tyrosinase reveal copper plasticity, J. Mol. Biol. 405 (2011) 227.
[26] D. Nokinsee, L. Shank, V.S. Lee, P. Nimmanpipug, Estimation of inhibitory effect against tyrosinase activity through homology modeling and molecular docking, Enzyme Res. 15 (2015) 1–12.
[27] X. Lai, H.J. Wichers, M. Soler-Lopez, B.W. Dijkstra, Structure of human tyrosinase related protein 1 reveals a binuclear zinc active site important for melanogenesis, Angew Chem Int Ed Engl. 56 (2017) 9812–9815.
[28] V. Vichai, K. Kirtikara, Sulforhodamine B colorimetric assay for cytotoxicity screening, Nat. Protoc. 1 (2006) 1112–1116.